6-4-

USNRDL-TR-654
13 May 1963

SUPPLEMENTARY ESTIMATES OF RADIATION GEOMETRY AND
ENERGY RESPONSE FOR USNRDL GAMMA-INTENSITY-TIME
RECORDER (GITR) MODEL 103

by
H. R. Rinnert

U.S. NAVAL RADIOLOGICAL
DEFENSE LABORATORY

SAN FRANCISCO 24, CALIFORNIA

TECHNICAL DEVELOPMENTS BRANCH
P. D. LaRiviere, Head

CHEMICAL TECHNOLOGY DIVISION
L. H. Gevantman, Head

ADMINISTRATIVE INFORMATION

This work was part of a project sponsored by the Office of Civil Defense and by the Defense Atomic Support Agency. The project is described in USNRDL Technical Program Summary for Fiscal Years 1963, 1964, and 1965, 1 November 1962, where it is designated Problem 13, Program A-1.

AVAILABILITY OF COPIES

Requests for additional copies by agencies or activities of the Department of Defense, their contractors certified to DDC (formerly ASTIA), and other government agencies or activities should be directed to the Defense Documentation Center for Scientific and Technical Information, Arlington Hall Station, Attn: TIPCR, Arlington 12, Virginia.

All other persons and organizations should direct requests for this report to the U. S. Department of Commerce, Office of Technical Services, Washington 25, D. C.

Eugene P. Cooper

Eugene P. Cooper
Scientific Director

E. B. Roth, CAPT USN
Commanding Officer and Director

12ND NRDL P1 (3-63)

ABSTRACT

Estimates of radiation response are presented for the Model 103 Gamma-Intensity-Time Recorder (GITR) as used at Operation Sunbeam. The GITR detector unit, consisting of two concentric ionization chambers, was mounted inside the GITR recorder case and located 3 ft above ground level. GITR responses and their time-dependence were estimated for several idealized radiation source geometries and several calculated gamma energy spectra. Estimated response values are presented as fractions of the GITR's calibration-response to Cs^{137} radiation beamed at the top of the unmounted detector along its longitudinal axis.

The principal conclusions drawn were that:

(1) The GITR responses to distributed sources with specified gamma energy spectra did not show a significant dependence upon the source geometries investigated.

(2) There were about 17 % differences between the responses of the two concentric detectors.

(3) The responses changed about 15 % during the first 100 hours after fission.

(4) The use of overall average GITR responses for distributed sources seems warranted; there is 95 % confidence that 95 % of the population of GITR responses will be within 12 % of the overall average response of 1.16 for the high-range detector, and within 14% of the overall average response of 0.99 for the low-range detector, during the first 110 hours after fission.

Because these response values are measures of the bias in the GITR calibration technique, the bias can be corrected (or at least minimized) by dividing the recorded GITR data by the above-mentioned overall average GITR response values.

SUMMARY

Problem

The Gamma-Intensity-Time Recorder (GITR) is calibrated by standardizing the response of unmounted detectors to radiation having only one energy and direction of incidence. This results in biased dose or dose rate data because the GITR response to gamma radiation depends upon the directions and energies of the incident radiation and upon the shielding provided by different types of GITR installations. Previous estimates of GITR response had been based upon radiological environments and shielding encountered aboard ships at sea. It was considered desirable to make additional estimates of response which would be more appropriate to the radiological environments encountered over large land areas, for GITR's which have their detectors mounted inside the recorder case.

Findings

The estimates of GITR response to radiation representative of fission products and induced activities did not show a significant dependence upon the geometries of the distributed radiation-sources investigated and showed only a minor dependence upon time after fission. For the conditions appropriate to Operation Sunbeam, it was estimated that the low-range detector is unbiased but that dose or dose rate data obtained with the high-range detector will be about 16 % too high.

1. INTRODUCTION

The evaluation and interpretation of dose or dose rate measurements requires some knowledge about how the measuring instrument responds to the radiation incident upon it. The instrument under consideration is the Model 103 Gamma-Intensity-Time Recorder (GITR) as used for Operation Sunbeam. The GITR detection unit, consisting of two concentric ionization chambers of different sensitivities, was mounted inside the GITR case (see Fig. 1.1) and positioned 3 ft above ground level. Detailed descriptions of the Model 103 GITR may be found in Reference 1.

1.1 Background

It had been shown[1] that the response of the Model 103 GITR to gamma radiation depends upon the directions and energies of the incident photons and upon the shielding provided by different types of GITR installations. There have also been previous presentations[1] of estimated GITR responses to several gamma energy spectra and radiation-source geometries applicable to Model 103 GITR's as used aboard test ships at Operation Hardtack.

However, the above mentioned esimates of response were derived:

(1) without consideration of plane radiation-sources, the principal source geometry for land areas;
(2) with the use of a rather random mixture of calculated and measured gamma energy spectra representing a somewhat narrow time span, which leaves some uncertainty as to how much the GITR responses may change with time;
(3) with consideration of absorption and photon energy degradation caused by penetration of radiation through 1-inch-thick steel, a consideration not appropriate to free-field measurements over land areas;
(4) but without consideration of photon energy degradation caused by Compton scattering in air, a consideration which may become important for free-field measurements over large land areas when other shielding media are absent.

Consequently, it was considered to be desirable to make some additional estimates of Model 103 GITR response which would be more appropriate to the radiological environments encountered at Operation Sunbeam.

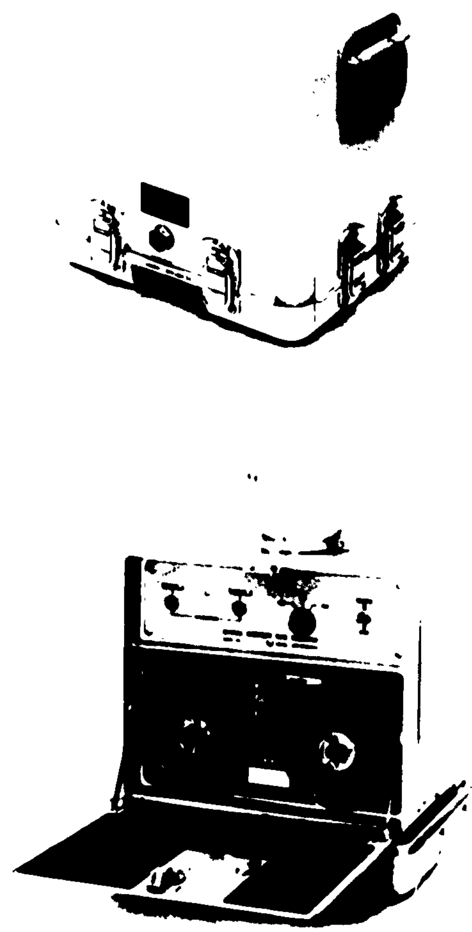

Fig. 1.1 The GITR Model 103 With and Without the Outer Water-tight Case Cover. The detector unit is shown mounted on the main instrument assembly.

1.2 Objective

The objective of this work was to determine - using existing GITR response data* - how, and to what extent, estimates of Model 103 GITR response depend upon the choice of time after fission, the radiation-source geometries, and the radiation energies assumed.

1.3 Approach

The GITR responses were to be evaluated for the following conditions:

(1) The GITR detector unit is mounted inside the recorder case and is positioned 3 ft above ground level.
(2) Calculated gamma energy spectra for the first 110 hr after fission are used to represent unscattered radiation from unfractionated fission products and from fission products plus induced activities. Additional calculated spectra represent radiation having degraded energies resulting from Compton scattering of photons in the air between source and detector.
(3) Radiation-source geometries are idealized. Actual directions of incidence for air-scattered photons are replaced by two extreme simplifications -- the directions of scattered photons are assumed to be unchanged by the degradation process, or all directions of scattered photons are assumed to be equally likely.
(4) Distributed radiation-sources are represented by hemispherical air volumes and by planes 3 ft below the detector.

The sequence of the investigation, also reflected in the sequence of presented results, was about as follows:

The existing response data were used to prepare normalized estimates of response to point-source radiation for various photon energies and directions of incidence (see Section 2). The normalization was chosen so that these basic response values indicated the bias existing in the GITR calibration technique.

Next, for each of the photon energies considered, geometry-weighted responses to mono-energetic radiation were calculated for several idealized source geometries by taking weighted averages of the basic point-source responses (see Section 3.1). The geometry-weighting-factors are derived in Appendix A.

Then, for each of the distributed radiation source geometries of interest, energy-and-geometry-weighted responses were calculated for

*Original data obtained by H. A. Zagorites of USNRDL, co-author of Reference 1.

various gamma energy spectra by taking weighted averages of the geometry-weighted responses mentioned above (see Section 3.2). The energy-weighting factors are derived in Appendix B.

Finally, the GITR responses were averaged - both overall and as a function of time - and various estimates of uncertainty were calculated (see Section 3.3).

2. AVERAGE RESPONSES TO POINT RADIATION-SOURCES

During the GITR response measurements, the GITR case (with the detectors mounted inside) had been rotated in three longitudinal planes (45 degrees apart) about the center of the detector unit.[1] The three response values for each of 17 vertical angles of radiation incidence (11.25 degrees apart) were averaged for each of five nominal gamma energies (viz., 0.07, 0.12, 0.18, 0.66, and 1.25 Mev - see Fig. 2.1). These averages were then divided by the value of the GITR-calibration response to Cs^{137} radiation beamed at the top of the unmounted detector along its longitudinal axis.

The resulting fractions, designated F (θ,E), are the average point-source response values presented in Tables 1 and 2 as functions of vertical angle of radiation incidence, θ, and nominal gamma energy, E. Note that the values of F (θ,E), and all estimates of GITR response to be derived therefrom, will automatically indicate any bias which may exist in the GITR calibration technique. For example, when point-source radiation comes from the lower solid angle of 1-pi steradians (i.e., θ is between 120 and 180 degrees), the values of F (θ,E) have an extremely wide spread; ranging between 0.03 and 1.02 for the low-range detector, and between 0.02 and 1.16 for the high-range detector. However, when point-source radiation comes from the upper solid angle of 3-pi steradians (i.e., θ is between 0 and 120 degrees), the values of F (θ,E) have a much narrower spread; ranging between 0.74 and 1.19 for the low-range detector, and between 0.86 and 1.32 for the high-range detector. For this latter geometry, the values of F (θ,E) are within about 26 % of the assigned overall average GITR responses discussed in Section 3.3.

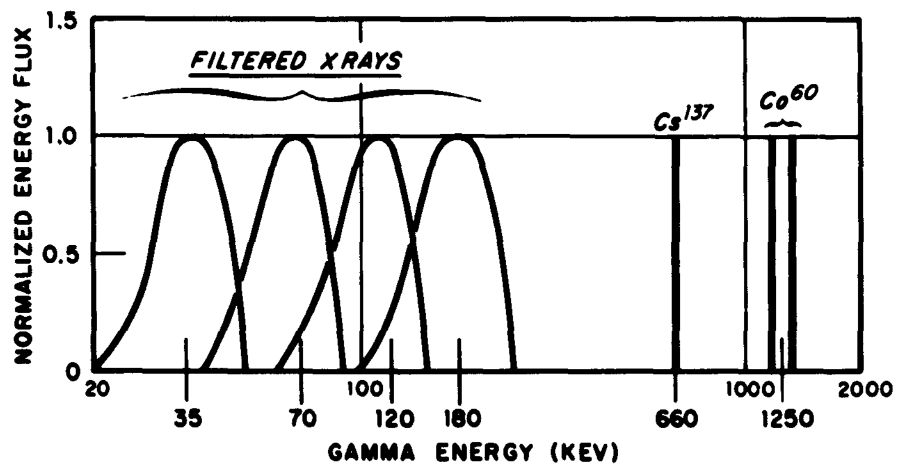

Fig. 2.1 Photon Energies of Radiation Used in Measurements of GITR Response. The lowest energy curve (viz., nominal 35-Kev X-Rays) does not apply to the Model 103 GITR.

TABLE 1

Average High Range Response (F) of Model 103 GITR (Detector Mounted Inside Case) To Point Sources of Specified Gamma Energy and Direction

Responses for 3 horizontal directions (45 degrees apart) were averaged for each vertical angle of radiation incidence. Values are fractions of calibration response to Cs^{137} beamed at top of unmounted detector along its longitudinal axis. $\theta = 0$ for radiation arriving from directly overhead.

Vertical Angle of Radiation Incidence, θ (degrees)	Nominal Gamma Energy (Mev)				
	0.07	0.12	0.18	0.66	1.25
0	0.9552	0.8568	0.9259	0.9638	1.0791
11	0.9937	0.9012	0.9737	1.0470	1.1416
22	1.0338	0.9478	1.0240	1.1373	1.2077
34	0.9383	0.9359	1.0172	1.1502	1.2151
45	0.9447	0.9242	1.0105	1.1633	1.2225
56	1.0491	0.9999	1.0556	1.1907	1.2434
67	1.1650	1.0816	1.1027	1.2187	1.2647
78	1.2185	1.1293	1.1248	1.2367	1.2771
90	1.2743	1.1788	1.1472	1.2549	1.2896
101	1.1962	1.1236	1.1110	1.2502	1.3163
112	0.9957	0.9937	1.0146	1.1821	1.2919
123	0.6148	0.7448	0.7959	1.0235	1.1590
135	0.3578	0.5524	0.6379	0.9102	1.0761
146	0.2205	0.3933	0.4947	0.7345	0.9363
157	0.0533	0.1534	0.2354	0.4553	0.6459
169	0.0361	0.1015	0.1409	0.3385	0.4295
180	0.0245	0.0672	0.0843	0.2517	0.2855

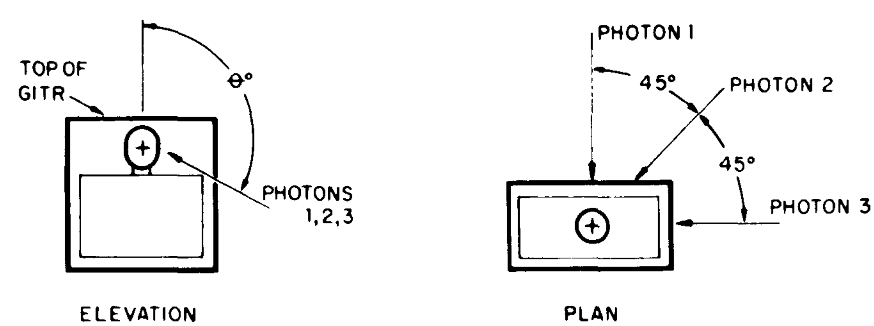

TABLE 2

Average Low Range Response (F) of Model 103 GITR (Detector Mounted Inside Case) To Point Sources of Specified Gamma Energy and Direction

Responses for 3 horizontal directions (45 degrees apart) were averaged for each vertical angle of radiation incidence. Values are fractions of calibration response to Cs^{137} beamed at top of unmounted detector along its longitudinal axis. θ = 0 for radiation arriving from directly overhead.

Vertical Angle of Radiation Incidence, θ (degrees)	Nominal Gamma Energy (Mev)				
	0.07	0.12	0.18	0.66	1.25
0	1.0546	0.8299	0.7691	0.9358	1.0948
11	1.0168	0.8262	0.7680	0.9494	1.1047
22	0.9823	0.8225	0.7668	0.9632	1.1148
34	0.9796	0.8416	0.7750	0.9712	1.1147
45	0.9769	0.8611	0.7832	0.9793	1.1146
56	1.0270	0.8961	0.7949	0.9855	1.1136
67	1.0796	0.9325	0.8068	0.9917	1.1125
78	1.1328	0.9524	0.8185	1.0051	1.1243
90	1.1887	0.9726	0.8303	1.0186	1.1361
101	1.1655	0.9592	0.8208	1.0092	1.1307
112	0.9740	0.8256	0.7368	0.9473	1.0829
123	0.7028	0.6333	0.6237	0.8693	1.0212
135	0.4214	0.4858	0.5063	0.7826	0.9553
146	0.2404	0.2238	0.3244	0.6414	0.8457
157	0.0572	0.0851	0.1386	0.4006	0.5794
169	0.0422	0.0824	0.1207	0.3604	0.5330
180	0.0311	0.0798	0.1051	0.3242	0.4903

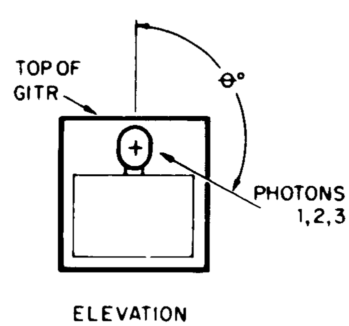

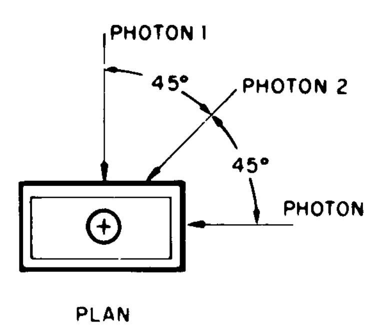

3. RESPONSES TO DISTRIBUTED RADIATION SOURCES

The GITR responses to distributed radiation sources having specific gamma energies were obtained by taking geometry-weighted averages of the point-source responses. In turn, the GITR responses to distributed sources having specified gamma energy spectra were obtained by taking energy-weighted averages of the geometry-weighted GITR responses.

3.1 Radiation Sources With Specific Gamma Energies

Geometry-weighted GITR responses, designated $G_j(E)$, to distributed radiation-sources having geometry j and gamma energy E were calculated from equations of the form

$$G_j(E) = \sum^{\Theta} S_j\ (\Theta,E)\ F\ (\Theta,E);$$

where the $S_j(\Theta,E)$ are geometry weighting factors, the $F(\Theta,E)$ are the point-source responses, and the summation covers the range of vertical angle of radiation incidence, Θ, appropriate to source geometry j. The geometry weighting factors, derived and presented in Appendix A, are estimates of the fraction of the dose rate contributed by radiation arriving from particular directions.

The specific designations of the $G_j(E)$ are defined as follows: G_h represents the response to hemispherical sources overhead when a finite source is so close that scattered radiation is insignificant or when it is assumed that scattered radiation from an infinite source has kept its initial direction of emission. G_s, which is actually the response to unscattered radiation from a spherical source all around the GITR, is used to represent the response to scattered radiation for which all directions of radiation incidence are assumed to be equally likely. G_{pf} represents the response to a finite plane source 3 ft below the detector. G_{pu} represents the response to unscattered radiation from an infinite plane source 3 ft below the detector. Finally, G_{ps} represents the response to scattered radiation from an infinite plane source 3 ft below the detector if it is assumed that the scattered radiation has kept its initial direction of emission.

The values of these weighted responses are presented in Table 3 for the various gamma energies E. Values of response range between 0.68 and 1.29, and for a given geometry the responses to different gamma energies may vary up to 53 %.

TABLE 3

Response (G) of Model 103 GITR to Radiation From Distributed Sources Having Specific Gamma Energies

Values are fractions of GITR-calibration response to Cs^{137} beamed at top of unmounted detector along its longitudinal axis. All estimates are based upon stipulation that energies and directions of photon incidence at detector are identical to energies and directions of photon emission from source.

Nominal Gamma Energy (Mev)	Plane Source 3 ft Below: Infinite		Plane Source 3 ft Below: 61 ft Dia.	Hemispherical Source Overhead	Spherical Source Around
	G_{pu}	G_{ps}	G_{pf}	G_h	G_s
	Unscattered Radiation Only	Scattered Radiation Only	Either Scattered or Unscattered Radiation		
			High-Range Detector		
0.07	1.019	1.257	0.878	1.100	0.907
0.12	1.004	1.168	0.896	1.031	0.900
0.18	1.011	1.139	0.919	1.070	0.938
0.66	1.172	1.252	1.100	1.192	1.095
1.25	1.248	1.289	1.207	1.245	1.182
			Low-Range Detector		
0.07	0.989	1.177	0.879	1.057	0.890
0.12	0.837	0.965	0.753	0.902	0.768
0.18	0.741	0.826	0.681	0.798	0.696
0.66	0.956	1.016	0.902	0.988	0.909
1.25	1.089	1.134	1.043	1.118	1.050

3.2 Radiation Sources With Specified Energy Spectra

Energy-and-geometry-weighted GITR responses, designated $H(j,i,t)$, to distributed radiation-sources having geometry j and energy spectrum i at time t were calculated from equations of the form

$$H = \sum_{u}^{E} \sum_{s}^{E} W_j(i,t,E)\ G_j\ (E).$$

The $W_j\ (i,t,E)$ are energy-weighting factors, the $G_j\ (E)$ are geometry-weighted GITR responses for specific energies E, and the summation covers contributions by unscattered (u) photons and, if applicable, by scattered (s) photons as well. The energy-weighting factors, derived and presented in Appendix B, are estimates of the fraction of the dose rate contributed by particular gamma energy intervals represented by E.

The specific designations and calculations of H are detailed below.

(1) For finite radiation sources (i.e., considering unscattered photons only):

$$H\ (h,i,t) = \sum^{E} W_u\ (i,t,E)\ G_h\ (E),$$

for a finite hemispherical source overhead;

$$H\ (pf,i,t) = \sum^{E} W_u\ (i,t,E)\ G_{pf}\ (E),$$

for a finite plane source 3 ft below.

(2) For infinite radiation sources (when it is assumed that scattered photons have not changed their initial directions of emission - nc = no change):

$$H(v,i,t)_{nc} = \sum^{E} W_{vu}\ (i,t,E)\ G_h\ (E) + \sum^{E} W_{vs}\ (i,t,E)\ G_h\ (E),$$

for an infinite volume source overhead;

$$H\ (p,i,t)_{nc} = \sum^{E} W_{pu}\ (i,t,E)\ G_{pu}\ (E) + \sum^{E} W_{ps}\ (i,t,E)\ G_{ps}\ (E),$$

for an infinite plane source 3 ft below.

(3) For infinite radiation sources (when it is assumed that all directions of incidence for scattered photons are equally likely - ss = spherical symmetry):

$$H\ (v,i,t)_{ss} = \sum^{E} W_{vu}\ (i,t,E)\ G_h(E) + \sum^{E} W_{vs}(i,t,E)\ G_s\ (E),$$

for an infinite volume source overhead;

$$H\ (p,i,t)_{ss} = \sum^{E} W_{pu}(i,t,E)\ G_{pu}(E) + \sum^{E} W_{ps}\ (i,t,E)\ G_s\ (E),$$

for an infinite plane source 3 ft below.

The several estimates of geometry-and-energy-weighted GITR response to distributed radiation-sources having various gamma energy spectra are presented in Tables 4 and 5, in addition to a few estimates of response to horizontally incident point-source "initial" radiation. For the low-range detector, the weighted responses range between 0.89 and 1.12 for hemispherical or volume sources overhead, and between 0.85 and 1.09 for plane sources below. For the high-range detector, the weighted responses range between 1.02 and 1.25 for hemispherical or volume sources overhead, and between 1.03 and 1.25 for plane sources below. These values show no significant dependence upon the geometries of the distributed sources investigated but they do show a slight dependence upon the change of energy spectra with time after fission.

3.3 Averages and Confidence Limits

Using the results shown in Tables 4 and 5, all responses for a given detector and given time after fission were averaged, and 95 % confidence limits were calculated (assuming normal populations of response values). These averages are presented in Table 6 and Fig. 3.1. The figure shows that there are differences of about 17 % in the responses of the two detectors and that these responses change about 15 % in the first 100 hr after fission. These differences, although statistically significant, are not very large.

Consequently, all the responses for each detector were averaged and are presented (with their 95 %-95 % Tolerance Limits) at the bottom of Table 6. Assuming normal populations, we have 95 % confidence that 95 % of the population of GITR response values will be within 12 %

TABLE 4

High Range Response (H) of Model 103 GITR (Detector Mounted Inside Case) to Specified Gamma Energy Spectra and Radiation Source Geometries

Values are fractions of calibration response to Cs^{137} radiation beamed at top of unmounted detector. U = Undegraded; D = Degraded; E = Energy; (FP) = Fission product spectrum; (FPIA) = Combined fission product and induced activity spectrum; SS assumes spherical symmetry for scattered radiation; NC assumes no change in direction for scattered radiation.

Spectrum and Geometry	Nominal Time After Fission (hr) ~0	0.1	1	5	11	24	51	110
				HEMISPHERICAL SOURCE OVERHEAD (HSO)				
UE > 0.9 Mev	1.245	-	-	-	-	-	-	-
U(FP)	-	1.237	1.221	1.208	1.204	1.195	1.187	1.190
U(FPIA)	-	1.233	1.216	1.202	1.194	1.177	1.153	1.140
D(FP)SS	-	1.151	1.124	1.106	1.100	1.083	1.070	1.078
D(FP)NC	-	1.203	1.186	1.174	1.170	1.159	1.151	1.157
D(FPIA)SS	-	1.142	1.115	1.098	1.086	1.061	1.032	1.022
D(FPIA)NC	-	1.200	1.182	1.170	1.162	1.147	1.131	1.126
HSO Ave.	1.245	1.194	1.174	1.160	1.153	1.137	1.121	1.119
				PLANE SOURCE 3 FT BELOW (PSB) Finite Diameter = 61 ft				
UE > 0.9 Mev	1.207	-	-	-	-	-	-	-
U(FP)	-	1.193	1.161	1.136	1.129	1.112	1.097	1.103
U(FPIA)	-	1.182	1.149	1.127	1.114	1.086	1.049	1.031
				Infinite Diameter				
UE > 0.9 Mev	1.248	-	-	-	-	-	-	-
D(FP)SS	-	1.205	1.176	1.155	1.150	1.134	1.117	1.116
D(FP)NC	-	1.240	1.219	1.205	1.200	1.190	1.184	1.191
D(FPIA)SS	-	1.184	1.163	1.147	1.135	1.109	1.074	1.055
D(FPIA)NC	-	1.236	1.216	1.200	1.192	1.177	1.161	1.157
PSB Ave.	1.228	1.207	1.191	1.162	1.153	1.135	1.114	1.109

HORIZONTAL RADIATION INCIDENCE FROM POINT SOURCE
UE > 0.9 Mev immediately after zero time

Horizontal Angle of Radiation Incidence is		Response is
normal to narrow side of GITR case		1.311
normal to wide side of GITR case		1.368
45° from above-mentioned normals		1.189
Unknown	Ave.	1.289

TABLE 5

Low Range Response (H) of Model 103 GITR (Detector Mounted Inside Case) to Specified Gamma Energy Spectra and Radiation Source Geometries

Values are fractions of calibration response to Cs^{137} radiation beamed at top of unmounted detector. U = Undegraded; D = Degraded; E = Energy; (FP) = Fission product spectrum; (FPIA) = Combined fission product and induced activity spectrum; SS assumes spherical symmetry for scattered radiation; NC assumes no change in direction for scattered radiation.

Spectrum and Geometry	Nominal Time After Fission (hr) ~0	0.1	1	5	11	24	51	110
				HEMISPHERICAL SOURCE OVERHEAD (HSO)				
UE > 0.9 Mev	1.118	-	-	-	-	-	-	-
U(FP)	-	1.105	1.066	1.037	1.029	1.010	0.999	1.012
U(FPIA)	-	1.105	1.064	1.030	1.016	0.990	0.961	0.952
D(FP)SS	-	1.009	0.974	0.950	0.942	0.921	0.907	0.921
D(FP)NC	-	1.055	1.029	1.008	1.002	0.986	0.976	0.989
D(FPIA)SS	-	1.010	0.970	0.944	0.932	0.910	0.890	0.890
D(FPIA)NC	-	1.062	1.029	1.005	0.998	0.984	0.975	0.980
HSO Ave.	1.118	1.058	1.022	0.996	0.987	0.967	0.951	0.957
				PLANE SOURCE 3 FT BELOW (PSB) Finite Diameter = 61 ft				
UE > 0.9 Mev	1.043	-	-	-	-	-	-	-
U(FP)	-	1.028	0.986	0.954	0.945	0.923	0.909	0.921
U(FPIA)	-	1.024	0.980	0.945	0.929	0.897	0.860	0.846
				Infinite Diameter				
UE > 0.9 Mev	1.089	-	-	-	-	-	-	-
D(FP)SS	-	1.046	1.005	0.976	0.968	0.947	0.933	0.944
D(FP)NC	-	1.072	1.037	1.013	1.005	0.988	0.984	1.001
D(FPIA)SS	-	1.037	1.000	0.968	0.954	0.927	0.898	0.891
D(FPIA)NC	-	1.077	1.039	1.008	0.997	0.978	0.966	0.970
PSB Ave.	1.066	1.047	1.008	0.977	0.966	0.943	0.925	0.929

HORIZONTAL RADIATION INCIDENCE FROM POINT SOURCE
UE > 0.9 Mev immediately after zero time

When Horizontal Angle of Radiation Incidence is	Response is
normal to narrow side of GITR case	1.145
normal to wide side of GITR case	1.195
45° from above-mentioned normals	1.069
Unknown	Ave. 1.136

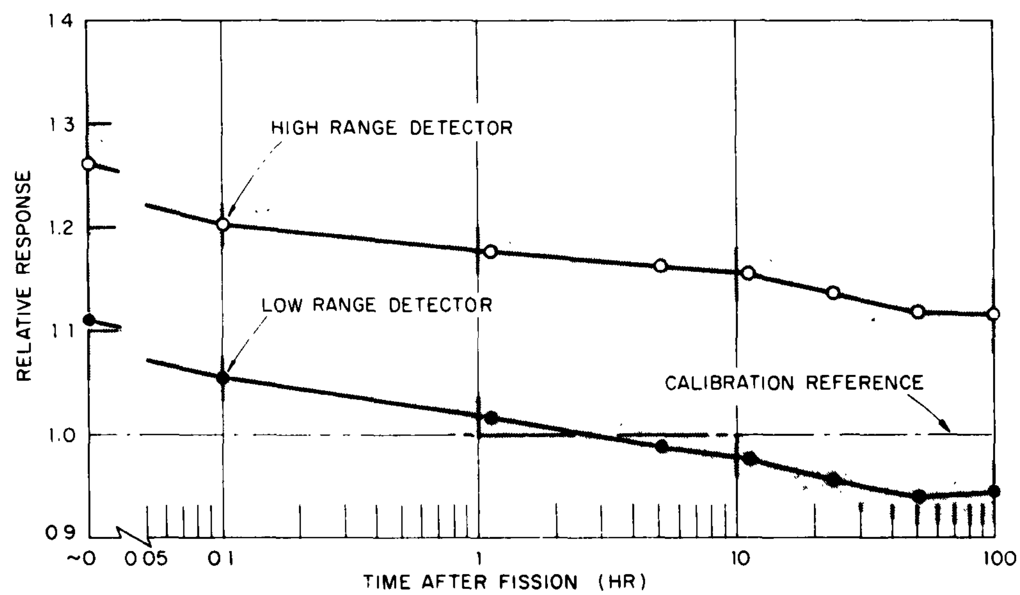

Fig. 3.1 Ninety-five Percent Confidence Region for Average Response of Model 103 GITR (detector mounted inside case) to Several Gamma Energy Spectra and Radiation Source Geometries as a Function of Time. Relative responses are fractions of calibration response to Cs^{137} beamed at top of unmounted detector.

TABLE 6

Average Response of Model 103 GITR (Detector Mounted Inside Case) to a Range of Gamma Energy Spectra and Radiation Source Geometries

Values are fractions of calibration response to Cs^{137} radiation beamed at top of unmounted detector. The averages were based upon all response values for all spectra and geometries presented in Tables 4 and 5.

Time After Fission (hr)	95 % Confidence Limits High-range Detector	95 % Confidence Limits Low-range Detector
	FOR AVERAGE RESPONSE VALUES	
~ 0	1.261 ± 0.070	1.110 ± 0.058
0.1	1.201 ± 0.021	1.053 ± 0.021
1.1	1.177 ± 0.023	1.015 ± 0.021
5.2	1.161 ± 0.025	0.987 ± 0.022
11.1	1.153 ± 0.026	0.976 ± 0.022
23.8	1.136 ± 0.029	0.955 ± 0.024
51.1	1.117 ± 0.033	0.938 ± 0.028
110.0	1.114 ± 0.037	0.943 ± 0.032
	FOR 95 % OF POPULATION OF RESPONSE VALUES	
0-110	1.159 ± 0.133	0.990 ± 0.141

of the overall average response of 1.16 for the high-range detector, and within 14 % of the overall average response of 0.99 for the low-range detector, during the first 110 hr after fission.

In Reference 1 the average values of response range between 1.27 and 1.06 for the high-range detector and between 1.07 and 0.93 for the low-range detector. These values are in very good agreement with those shown in Fig. 3.1.

4. CONCLUSIONS

The GITR responses to point source radiation will be within about 26 % of the assigned overall average response to distributed sources if the direction of radiation incidence is within the upper solid angle of 3 pi steradians (i.e., θ is between 0 and 120 degrees). This implies that strict uniformity of contaminant distribution is not a critical requirement for use of an average GITR response applicable to transit radiation.

For a given geometry of distributed radiation sources the GITR response to different gamma energies may vary up to 53 %. However, all responses to mono-energetic distributed sources were within 31 % of the overall average GITR response assigned to each detector.

The GITR responses to distributed sources with specified gamma energy spectra did not show a significant dependence upon the source geometries investigated. However, there were about 17 % differences between the responses of the two detectors; and the responses changed about 15 % in the first 100 hr after fission because of changes in the spectra resulting from different rates of growth and decay for the several fission products and induced activities.

The use of overall average GITR responses to distributed sources seems warranted; there is 95 % confidence that 95 % of the population of GITR response values will be within 12 % of the assigned overall average response value of 1.16 for the high-range detector, and within 14 % of the assigned overall average response value of 0.99 for the low-range detector, during the first 110 hr after fission if the detectors are mounted inside the GITR case.

Because these response values are measures of the bias in the GITR calibration technique, the bias can be corrected (or at least minimized) by dividing the recorded GITR data by the above-mentioned overall average GITR response values.

REFERENCES

1. M. M. Bigger, et al. Shipboard Radiation From Underwater Bursts, Operation Hardtack, Project 2.1. DASA report WT-1619, Volume I, March 1961. (Confidential-FRD).

2. H. Goldstein, J. E. Wilkins Jr. Calculations of the Penetration of Gamma Rays. AEC Report NYO-3075, June 1954.

3. A. T. Nelms, J. W. Cooper. U^{235} Fission Product Decay Spectra at Various Times After Fission. National Bureau of Standards, NBS-5853, April 1958.

4. T. Rockwell. Reactor Shielding Design Manual. AEC Report TID-7004, March 1956.

5. E. R. Tompkins, L. B. Werner. Chemical, Physical, and Radiological Characteristics of the Contaminant, Operation Castle, Project 2.6a. DASA report WT-917, September 1955 (Secret-RD).

6. T. Triffet, P. D. LaRiviere. Characterization of Fallout, Operation Redwing Project 2.63. DASA report WT-1317, August 1958 (Secret-RD).

7. L. D. Gates Jr., C. Eisenhauer. Spectral Distribution of Gamma Rays Propagated in Air. AFSWP-502A, January 1954.

APPENDIX A

ESTIMATION OF SOURCE GEOMETRY WEIGHTING FACTORS

The weighting factors used for the estimation of GITR response to a specified source geometry were actually estimates of the fractions of the dose rate contributed by gamma radiation coming from particular directions.

The directions of radiation incidence for the unscattered radiation were easily defined by the assumed source geometries. However, the actual directions of incidence for the scattered radiation were not so easily handled - therefore, for simplicity's sake, two extreme conditions were assumed: (1) the scattered radiation did not change direction, i.e., directions were the same for scattered as for unscattered radiation; or (2) the scattered radiation came from all directions with equal likelihood, i.e., spherical symmetry was assumed.

For the following derivations let us define:

R is dose rate at point P, r/hr
k is dose rate one foot above a one-square-foot contaminated plane, r/hr per ft^2
K is dose rate one foot from a one-cubic-foot contaminated air volume, r/hr per ft^3
B is dose rate buildup factor due to scattered radiation, dimensionless
r is slant distance from point P to contaminated point source, ft
h is height of point P above contaminated plane, ft
X is horizontal distance between point P and contaminated point source, ft
θ is angle between vertical line and direction of radiation incidence at point P, degrees
μ is linear attenuation coefficient for air, per ft
$y=\mu r$ is number of mean-free-paths between point P and contaminated point source, dimensionless
a,b,c are constants
S is the fraction of the dose rate contributed by a particular region of a radiation source.

For plane sources:

$$dR = k\,(1/r^2)2\pi\, x \quad dx\ B \exp[-\mu r],$$
$$r^2 = x^2 + h^2,\ rdr = xdx$$
$$\therefore\ dR = 2\pi\, k\,(dr/r)B \exp[-\mu r]$$
$$\text{or } dR = 2\pi\, k\,(dy/y)B \exp[-y]$$

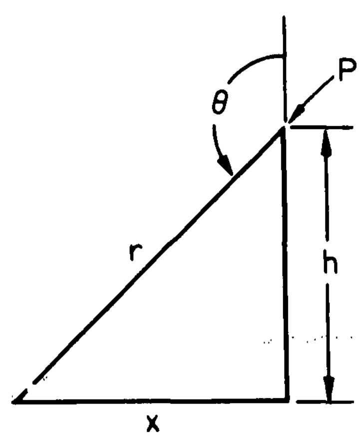

Now

$$dR = \overbrace{2\pi\, k\,(dy/y)\exp[-y]}^{\text{Unscattered Component}} + \overbrace{2\pi\, k\,(dy/y)(B-1)\exp[-y]}^{\text{Scattered Component}}$$

or the dose rate from an annular region defined by y_1 and y_2 is:

$$R\,(y_1,y_2) = 2\pi\, k \int_{y_1}^{y_2} (dy/y)e^{-y} + 2\pi\, k \int_{y_1}^{y_2} (dy/y)(B-1)\ e^{-y}.$$

The exponential integral $(-E_i\,[-y]\,) = \int_y^{\infty} (dy/y)\,e^{-y}$,

therefore the dose rate from unscattered radiation coming from the annular region is

$$R\,(y_1,y_2)_{unscattered} = 2\pi\,k\left\{(-E_i\,[-y_1] - (-E_i\,[-y_2])\right\};$$

and the fractional contribution is

$$S\,(y_1,y_2)_{unscattered} = \left\{\frac{R\,(y_1,y_2)_{unscattered}}{R\,(y_{minimum},y_{maximum})_{unscattered}}\right\}$$

Now let $B = 1 + ay + by^2 + cy^3$ where a, b, and c are evaluated for various energies by using the buildup factors (for homogeneous infinite media) obtained from Reference 2. Then the dose rate contributed by scattered radiation coming from the annular region (assuming no changes in direction) is

$$R\,(y_1,y_2)_{scattered} = 2\pi\,k\int_{y_1}^{y_2} (ay + by^2 + cy^3)(dy/y)\,e^{-y}$$

$$\text{or}\quad R\,(y_1,y_2)_{scattered} = 2\pi\,k\left\{e^{-y_1}([a+b+2c] + [b+2c]\,y_1 + cy_1^2) - e^{-y_2}([a + b + 2c] + [b + 2c]\,y_2 + cy_2^2)\right\};$$

and the fractional contribution is

$$S(y_1,y_2)_{scattered} = \left\{\frac{R\,(y_1,y_2)_{scattered}}{R\,(y_{minimum},y_{maximum})_{scattered}}\right\}.$$

For spherical or hemispherical sources:

$$dR = K(1/r^2)(2\pi\,r\,\sin\Theta)\,rd\Theta dr\;B\,\exp\,[-\mu r]$$

$$\text{or}\quad dR = 2\pi K\,(\sin\Theta\,d\Theta)(B\,\exp\,[-\mu r]\,dr).$$

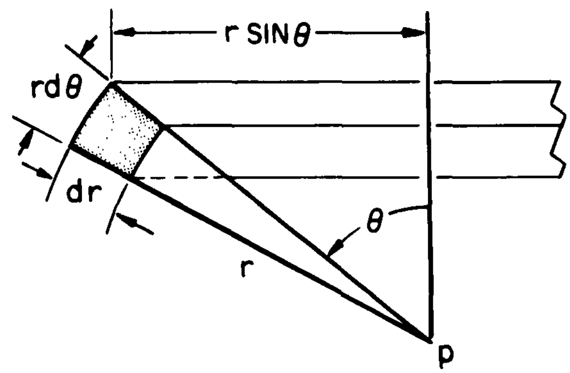

For a spherical source - used only for the assumption that scattered radiation comes from all directions with equal probability - the dose rate increment is

$$(dR)_{scattered} = 2\pi\ K\ (\sin\theta d\theta)\left\{(B-1)\ \exp[-\mu r]\ dr\right\} .$$

For a hemispherical source the unscattered component is

$$(dR)_{unscattered} = 2\pi\ K\ (\sin\theta d\theta)\left\{\exp[-\mu r]dr\right\} \quad ;$$

and the scattered component - assuming no changes in direction - is

$$(dR)_{scattered} = 2\pi\ K\ (\sin\theta d\theta)\left\{(B-1)\ \exp\ [-\mu r]\ dr\right\} .$$

Since all three equations are of the form

$$dR = 2\pi\ K\ (\sin\theta d\theta)(A\ \exp\ [-\mu r]\ dr),$$

where A is either 1 or (B-1), the dose rate contributed by a particular region defined by Θ_1, Θ_2, r_1, and r_2 is

$$R(\Theta_1,\Theta_2,r_1,r_2) = 2\pi K \int_{r_1}^{r_2}\int_{\Theta_1}^{\Theta_2} A(\exp[-\mu r])(\sin\Theta\, d\Theta)dr$$

$$= 2\pi K\,[\cos\Theta_1-\cos\Theta_2]\int_{r_1}^{r_2} A \exp[-\mu r]\, dr,$$

and the fractional dose rates - for a spherical or hemispherical shell whose thickness is defined by r_1 and r_2 - are

$$S(\Theta_1,\Theta_2,r_1 r_2) = \left\{\frac{[\cos\Theta_1 - \cos\Theta_2]\int_{r_1}^{r_2} A \exp[-\mu r]\, dr}{[\cos(\Theta_{minimum})-\cos(\Theta_{maximum})]\int_{r_1}^{r_2} A \exp[-\mu r]\, dr}\right\}$$

Since the integrals in the numerator and in the denominator are equal, the expression simplifies to

$$S(\Theta_1,\Theta_2,r_1,r_2) = S(\Theta_1,\Theta_2) = \left\{\frac{\cos\Theta_1 - \cos\Theta_2}{\cos(\Theta_{minimum})-\cos(\Theta_{maximum})}\right\}$$

which is independent of the shell thickness. Consequently, these values of $S(\Theta_1,\Theta_2)$ are also used to estimate the dose rate contributions from infinite volume sources.

In all cases, for either plane or volume sources, the fractional dose rates have been defined so that

$$\sum_{y_{minimum}}^{y_{maximum}} S(y_1,y_2) = \sum_{\Theta_{minimum}}^{\Theta_{maximum}} S(\Theta_1,\Theta_2) = 1.$$

The various source-geometry weighting factors, S, - corresponding to the angles of radiation incidence for which GITR responses had been measured - were actually calculated for gamma radiation energies of

0.255, 0.5, 1, and 2 Mev because build-up factors for these (and higher) energies were available. These values of S were then plotted as a function of energy and curves were drawn so that, by interpolation and extrapolation, the values of S for the actual energies of interest could be estimated.

The results of the above-mentioned calculations and estimations are presented in Tables A.1 and A.2. The finite plane (with its 61 ft maximum diameter) was created by simply eliminating the annular region represented by the nominal vertical angle of radiation incidence $\theta = 90^{\circ}$; this was done purely for ease of calculation.

TABLE A.1

Estimated Fraction (S) of Dose Rate Contributed by Various Contaminated Annular Regions of a Plane 3 ft Below Detector

θ = 0 for radiation arriving from directly overhead.

Nominal Vertical Angle of Radiation Incidence, θ (degrees)	Radii of Annular Region (ft)	Gamma Energy of Radiation Source (Mev) 0.07	0.12	0.18	0.66	1.25
	UNSCATTERED Component From FINITE (61 ft dia.) Plane S_{pf}					
101	9.89 - 30.5	0.4488	0.4510	0.4528	0.4585	0.4607
112	5.61 - 9.89	0.2130	0.2126	0.2122	0.2109	0.2102
123	3.66 - 5.61	0.1332	0.1325	0.1319	0.1302	0.1299
135	2.46 - 3.66	0.0886	0.0882	0.0879	0.0869	0.0864
146	1.60 - 2.46	0.0591	0.0589	0.0588	0.0581	0.0577
157	0.91 - 1.60	0.0369	0.0367	0.0365	0.0360	0.0358
169	0.30 - 0.91	0.0183	0.0180	0.0178	0.0173	0.0172
180	0 - 0.30	0.0021	0.0021	0.0021	0.0021	0.0021
	UNSCATTERED Component From INFINITE Plane S_{pu}					
90	30.5 - ∞	0.3617	0.3853	0.4039	0.4643	0.4962
101	9.89 - 30.5	0.2819	0.2746	0.2687	0.2456	0.2321
112	5.61 - 9.89	0.1343	0.1315	0.1266	0.1128	0.1059
123	3.66 - 5.61	0.0863	0.0824	0.0775	0.0701	0.0654
135	2.46 - 3.66	0.0570	0.0545	0.0525	0.0466	0.0438
146	1.60 - 2.46	0.0380	0.0365	0.0350	0.0310	0.0290
157	0.91 - 1.60	0.0238	0.0227	0.0219	0.0192	0.0180
169	0.30 - 0.91	0.0117	0.0112	0.0106	0.0093	0.0085
180	0 - 0.30	0.0013	0.0013	0.0013	0.0011	0.0011
	SCATTERED Component From INFINITE Plane S_{ps} Assuming No Change in Direction for Scattered Radiation					
90	30.5 - ∞	0.9135	0.9224	0.9288	0.9456	0.9533
101	9.89 - 30.5	0.0633	0.0566	0.0520	0.0398	0.0341
112	5.61 - 9.89	0.0126	0.0113	0.0104	0.0079	0.0068
123	3.66 - 5.61	0.0053	0.0047	0.0043	0.0033	0.0028
135	2.46 - 3.66	0.0026	0.0024	0.0022	0.0017	0.0015
146	1.60 - 2.46	0.0015	0.0014	0.0013	0.0010	0.0008
157	0.91 - 1.60	0.0009	0.0009	0.0007	0.0005	0.0005
169	0.30 - 0.91	0.0004	0.0004	0.0003	0.0002	0.0002
180	0 - 0.30	0.0000	0.0000	0.0000	0.0000	0.0000

TABLE A.2

Estimated Fraction (S) of Dose Rate Contributed by Various Zones of A Contaminated Sphere or Hemisphere

θ = 0 for radiation arriving from directly overhead.

Nominal Vertical Angle of Radiation Incidence, θ (degrees)	Zone Boundaries θ_1, θ_2 (degrees)	Hemisphere Above Detector: UNSCATTERED or SCATTERED Radiation With no Change in Direction S_h	Sphere Around Detector: Used for Assumption of Spherical Symmetry for SCATTERED RADIATION S_s
0	0 - 6	0.0048	0.0024
11	6 - 17	0.0383	0.0191
22	17 - 28	0.0750	0.0375
34	28 - 39	0.1089	0.0545
45	39 - 51	0.1386	0.0693
56	51 - 62	0.1630	0.0815
67	62 - 73	0.1811	0.0906
78	73 - 84	0.1923	0.0961
90	84 - 90	0.0980	-
90	84 - 96	-	0.0980
101	96 - 107	-	0.0961
112	107 - 118	-	0.0906
123	118 - 129	-	0.0815
135	129 - 141	-	0.0693
146	141 - 152	-	0.0545
157	152 - 163	-	0.0375
169	163 - 174	-	0.0191
180	174 - 180	-	0.0024

APPENDIX B

ESTIMATION OF GAMMA ENERGY WEIGHTING FACTORS

The geometry-weighted responses to specific gamma energies, G, were in turn weighted by factors which are actually estimates of the fraction of the dose rate contributed by particular gamma energy intervals of a specified energy spectrum.

Gamma energy spectra change with time, due to the different rates of growth and decay for the several fission products and induced activities. Because measured spectral data for the first few hours after fission were rather limited in availability and detail, it was expedient to use calculated gamma energy spectra for the estimation of changes in GITR response due to changes in spectra with time.

B.1 Undegraded Fission Products

Unfractionated and undegraded source-spectra due to U^{235} fission products were based upon Table 2 of Reference 3. The tabulated values of photons/sec-Mev-10^4 fissions for each energy interval were multiplied by the width of the interval to obtain the number of photons/sec-10^4 fissions in the energy interval. Figure 2.1 of Reference 4 was then used to obtain factors (i.e., r/hr per photon/cm^2-sec) which converted the photon spectra into dose-rate spectra - the dose rates at 1 cm, (r/h ($4\pi \times 10^4$ fissions), contributed by the 19 to 22 energy intervals used i Reference 3. The dose rates for several of these intervals were combine and normalized to result in fractions of dose rate (W_u) contributed by the five intervals (viz., less than 0.09, 0.09-0.15, 0.15-0.35, 0.35-0.9 and greater than 0.9 Mev) representing the energies for which GITR response measurements had been made. All fractions W for 1.1 to 110 hours after fission had already been calculated for another report.* The fractions for 0.1 hour after fission, desired for this report, were estimated by extrapolating the curves of W vs time after fission.

*H. Rinnert. Estimates of Radiation Geometry and Energy Response for the USNRDL Model 1954-56 GITR. USNRDL-TR to be published.

B.2 Undegraded Fission Products and Induced Activities

The effects of induced activities were approximated as follows:

(1) Estimates of photon spectra (photons/sec-10^4 fissions, if capture-to-fission ratio is unity) for various possible induced activities were obtained* as functions of time.

(2) References 5 and 6 were used to obtain reported sets of capture-to-fission ratios for induced activities observed in actual fallout contaminants.

(3) Items (1) and (2) were then combined into several sets of induced activity photon spectra as functions of time.

(4) When, in each source-energy interval, the number of photons/sec-10^4 fissions for the various sets of induced activities were added to those for the fission products, it was noted that there was a general shift toward the lower energies. Because it was desired to estimate GITR responses for a wide range of energy spectra, the particular set of observed induced-activities spectra which (when combined with the calculated fission-products spectra) maximized the shift toward the low energies was selected for this study.

(5) The conversion of photons/sec-10^4 fissions to dose rate contributions (W_u) has already been described in Section B.1.

B.3 Degraded Spectra

In order to approximate the effect of energy degradation resulting from photon scattering by the intervening air between source and detector the techniques of Gates and Eisenhauer, explained in Reference 7, were used to estimate the degraded spectra applicable to an infinite volume source and to an infinite plane isotropic source 3 feet below the detector. In brief:

(1) Given $[D_i(E)]_j$ as the fraction of the dose or dose rate delivered by photons having energies less than or equal to E Mev from an infinite source having a specific source energy $E_o = E_j$. Esimates of $D_i(E)$ for various energies E and E_o are presented in Figures B.1 and B.2 (note - these figures are this author's revision of the actual figures in Reference 7.

(2) Given w_j as the fraction of the dose rate which would be contributed by the j^{th} source-energy interval of an infinite plane source if only unscattered photons were considered. To evaluate w_j let us define:

*Table II in: W. Williamson, H. Rugge. Gamma Spectra for Some Possible Induced Activities Accompanying a Nuclear Explosion. USNRDL-TM-106, 18 March 1959.

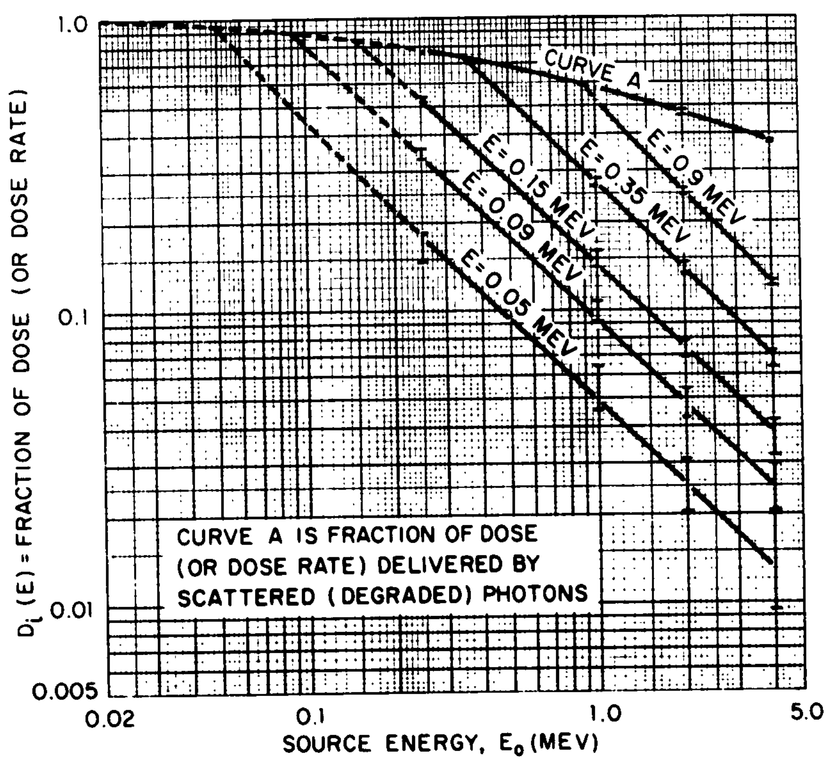

Fig. B.1 Estimated Fraction of Dose (or dose rate), $D_i(E)$, Delivered by Photons With Energy Less Than E Mev From Uniformly Distributed INFINITE VOLUME SOURCE of Source Energy E_0. This is a replot of Figure 11 in Reference 7.

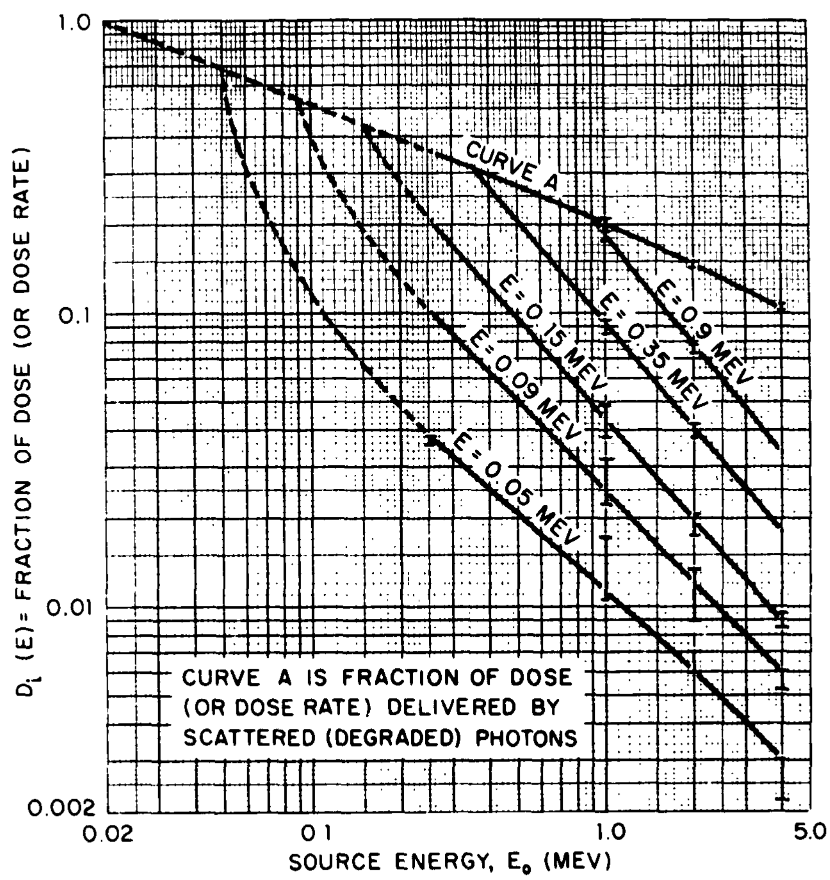

Fig. B.2 Estimated Fraction of Dose (or dose rate), $D_i(E)$, Delivered by Photons With Energy Less than E Mev Three Feet Above an INFINITE PLANE ISOTROPIC SOURCE of Source Energy E_0. This is a replot of Figure 20 in Reference 7.

P_j as the fraction of the gamma energy in the j^{th} source-energy interval (i.e., the P_j are the gamma source-energy spectrum);

$D_j(A)$ as the fraction of the dose rate delivered by <u>scattered</u> photons having original source energy $E_o = E_j$; see Curve A in Figures B.1 or B.2;

K_j as either the "true" linear absorption coefficient shown in Table 8 of Reference 7, or the mass energy-absorption coefficient shown on page 450 of Reference 4;

y_j as the height (in mean-free-paths of air) of the detector above the infinite plane source of energy E_j;

$(-E_i[-y])$ as the exponential integral representing $\int_y^{\infty} \frac{\exp[-s]}{s} ds$, where s is the slant distance (in mean-free-paths of air) between the detector and a point source in the plane.

Then, according to Reference 7,

$$w_j = \left\{\frac{P_j K_j(-E_i[-y_j])}{[1 - D_j(A)]}\right\} \Bigg/ \sum^{j} \left\{\frac{P_j K_j(-E_i[-y_j])}{[1 - D_j(A)]}\right\}$$

where the $D_j(A)$ are obtained from Figure B.2.

(3) Combining (1) and (2) above, the estimated fraction of the dose or dose rate, delivered by both scattered and unscattered photons having energies less than or equal to E Mev, from an infinite source with a source-energy spectrum defined by a set of P_j's is:

$D(E) = \sum^{j} P_j [D_i(E)]_j$ for an infinite air volume source, where the $[D_i(E)]_j$ are found in Figure B.1; and

$D(E) = \sum^{j} w_j [D_i(E)]_j$ for an infinite plane source three feet below the detector, where the $[D_i(E)]_j$ are found in Figure B.2.

(4) Now, it follows that the fraction of the dose rate (W) delivered by both scattered and unscattered photons having energies between E_1 and E_2 Mev is $W = D(E_2) - D(E_1)$.

The fraction of the dose rate delivered by unscattered photons having energies between E_1 and E_2 Mev is

$$Wvu = \sum_{E_1}^{E_2} P_j \, [1 - D_j(A)],$$ for infinite volume source, where the summation covers all source energy intervals included between E_1 and E_2 Mev and where $D_j(A)$ is found in Figure B.1, and

$$Wpu = \sum_{E_1}^{E_2} w_j \, [1 - D_j(A)],$$ for infinite plane source, where the summation covers all source energy intervals included between E_1 and E_2 Mev and where $D_j(A)$ is found in Figure B.2.

The fraction of the dose rate delivered by scattered photons having energies between E_1 and E_2 Mev is, therefore, simply the difference

$$W_{vs} = (W)_{volume} - W_{vu},$$ for volume sources;

$$W_{ps} = (W)_{plane} - W_{pu},$$ for plane sources.

B.4 Energy-Weighting Factors

The results of the above-mentioned calculations are presented as functions of time in Tables B.1 and B.2 for undegraded and degraded energy spectra, for fission products only, and for fission products plus induced activities.

TABLE B.1

Estimated Fraction of Dose Rate (W) Contributed by Various Gamma Energy Intervals of a Fission-Product Spectrum

Energy Interval (Mev)	Time After Fission (hr)						
	0.1	1.1	5.2	11.1	23.8	51.1	110
			UNDEGRADED SPECTRUM (W_u)				
< 0.09	0.0049	0.0080	0.0118	0.0110	0.0147	0.0296	0.0450
0.09 - 0.15	0.0088	0.0036	0.0017	0.0015	0.0029	0.0069	0.0120
0.15 - 0.35	0.0187	0.0398	0.0624	0.0704	0.0855	0.1020	0.1023
0.35 - 0.90	0.0344	0.2903	0.4564	0.4994	0.6091	0.6415	0.5246
> 0.90	0.9332	0.6583	0.4677	0.4177	0.2878	0.2200	0.3161
			DEGRADED SPECTRUM IN AIR 3 FT ABOVE INFINITE CONTAMINATED PLANE				
			Component due to UNSCATTERED Radiation (W_{pu})				
< 0.09	0.0026	0.0044	0.0065	0.0061	0.0082	0.0161	0.0237
0.09 - 0.15	0.0026	0.0023	0.0010	0.0021	0.0019	0.0043	0.0072
0.15 - 0.35	0.0141	0.0265	0.0417	0.0465	0.0571	0.0667	0.0642
0.35 - 0.90	0.0194	0.2152	0.3394	0.3718	0.4526	0.4646	0.3689
> 0.90	0.7740	0.5450	0.3853	0.3447	0.2359	0.1740	0.2446
			Component due to SCATTERED Radiation (W_{ps})				
< 0.09	0.0271	0.0442	0.0566	0.0552	0.0638	0.0950	0.1247
0.09 - 0.15	0.0126	0.0179	0.0214	0.0235	0.0268	0.0292	0.0276
0.15 - 0.35	0.0363	0.0470	0.0541	0.0571	0.0645	0.0677	0.0601
0.35 - 0.90	0.0484	0.0605	0.0682	0.0699	0.0741	0.0723	0.0633
> 0.90	0.0629	0.0370	0.0258	0.0231	0.0151	0.0101	0.0157
			DEGRADED SPECTRUM AT CENTER OF INFINITE CONTAMINATED VOLUME OF AIR				
			Component due to UNSCATTERED Radiation (W_{vu})				
< 0.09	0.0000	0.0000	0.0001	0.0001	0.0002	0.0006	0.0009
0.09 - 0.15	0.0014	0.0006	0.0003	0.0003	0.0005	0.0012	0.0021
0.15 - 0.35	0.0041	0.0092	0.0148	0.0165	0.0207	0.0256	0.0252
0.35 - 0.90	0.0412	0.0983	0.1634	0.1798	0.2240	0.2396	0.1935
> 0.90	0.4684	0.3546	0.2616	0.2350	0.1620	0.1195	0.1748
			Component due to SCATTERED Radiation (W_{vs})				
< 0.09	0.0665	0.0906	0.1063	0.1124	0.1305	0.1514	0.1523
0.09 - 0.15	0.0342	0.0475	0.0560	0.0595	0.0684	0.0753	0.0704
0.15 - 0.35	0.0853	0.1141	0.1304	0.1361	0.1531	0.1644	0.1501
0.35 - 0.90	0.1321	0.1622	0.1779	0.1800	0.1976	0.1864	0.1732
> 0.90	0.1668	0.1229	0.0892	0.0903	0.0530	0.0360	0.0575

TABLE B.2

Estimated Fraction of Dose Rate (W) Contributed by Various Gamma Energy Intervals of a Combined Fission Products and Induced Activity Spectrum

Energy Interval (Mev)	Time After Fission (hr) 0.1	1.1	5.2	11.1	23.8	51.1	110
	UNDEGRADED SPECTRUM (W_u)						
< 0.09	0.0500	0.0419	0.0118	0.0110	0.0150	0.0276	0.0425
0.09 - 0.15	0.0010	0.0053	0.0165	0.0315	0.0637	0.1228	0.1622
0.15 - 0.35	0.0190	0.0401	0.0738	0.0942	0.1362	0.2112	0.2641
0.35 - 0.90	0.0270	0.2852	0.4618	0.4924	0.5366	0.4691	0.3363
> 0.90	0.9030	0.6275	0.4361	0.3709	0.2485	0.1693	0.1949
	DEGRADED SPECTRUM IN AIR 3 FT ABOVE INFINITE CONTAMINATED PLANE Component due to UNSCATTERED Radiation (W_{pu})						
< 0.09	0.0268	0.0243	0.0065	0.0061	0.0082	0.0148	0.0219
0.09 - 0.15	0.0006	0.0033	0.0104	0.0198	0.0394	0.0731	0.0932
0.15 - 0.35	0.0069	0.0262	0.0490	0.0616	0.0886	0.1320	0.1577
0.35 - 0.90	0.0489	0.2077	0.3412	0.3628	0.3889	0.3264	0.2258
> 0.90	0.6972	0.5106	0.3579	0.3039	0.1998	0.1297	0.1445
	Component due to SCATTERED Radiation (W_{ps})						
< 0.09	0.0923	0.0734	0.0641	0.0711	0.0958	0.1479	0.1904
0.09 - 0.15	0.0092	0.0175	0.0248	0.0297	0.0387	0.0509	0.0567
0.15 - 0.35	0.0277	0.0451	0.0558	0.0595	0.0654	0.0671	0.0625
0.35 - 0.90	0.0332	0.0574	0.0664	0.0652	0.0623	0.0503	0.0380
> 0.90	0.0572	0.0345	0.0239	0.0203	0.0129	0.0078	0.0093
	DEGRADED SPECTRUM AT CENTER OF INFINITE CONTAMINATED VOLUME OF AIR Component due to UNSCATTERED Radiation (W_{vu})						
< 0.09	0.0034	0.0029	0.0002	0.0002	0.0004	0.0008	0.0012
0.09 - 0.15	0.0001	0.0008	0.0024	0.0045	0.0093	0.0180	0.0236
0.15 - 0.35	0.0032	0.0092	0.0174	0.0218	0.0321	0.0498	0.0610
0.35 - 0.90	0.0212	0.0963	0.1641	0.1751	0.1923	0.1676	0.1191
> 0.90	0.4538	0.3377	0.2439	0.2083	0.1385	0.0906	0.1045
	Component due to SCATTERED Radiation (W_{vs})						
< 0.09	0.1187	0.1230	0.1247	0.1478	0.1974	0.2750	0.3194
0.09 - 0.15	0.0299	0.0465	0.0598	0.0663	0.0786	0.0927	0.0971
0.15 - 0.35	0.0753	0.1106	0.1321	0.1376	0.1478	0.1477	0.1355
0.35 - 0.90	0.1033	0.1561	0.1722	0.1673	0.1578	0.1295	0.1042
> 0.90	0.1911	0.1169	0.0832	0.0711	0.0458	0.0283	0.0344

INITIAL DISTRIBUTION

NO. CPY	
	NAVY
3	CHIEF, BUREAU OF SHIPS (CODE 210L)
1	CHIEF, BUREAU OF SHIPS (CODE 320)
6	CHIEF, BUREAU OF SHIPS (CODE 685C)
1	CHIEF, BUREAU OF MEDICINE AND SURGERY
1	CHIEF OF NAVAL OPERATIONS (OP-07T)
1	CHIEF OF NAVAL RESEARCH (CODE 104)
1	COMMANDER, NEW YORK NAVAL SHIPYARD (MATERIAL LAB)
3	DIRECTOR, NAVAL RESEARCH LABORATORY (CODE 2021)
1	OFFICE OF NAVAL RESEARCH (CODE 422)
10	OFFICE OF NAVAL RESEARCH, FPO, NEW YORK
1	COMMANDER, NAVAL AIR MATERIAL CENTER, PHILADELPHIA
2	CHIEF, BUREAU OF SHIPS (CODE 210L)
1	NAVAL MEDICAL RESEARCH INSTITUTE
1	US NAVAL POSTGRADUATE SCHOOL, MONTEREY
1	OFFICE OF PATENT COUNSEL, SAN DIEGO
	ARMY
1	OFFICE OF CHIEF RESEARCH AND DEVELOPMENT (ATOMIC OFFICE)
1	CHIEF OF RESEARCH AND DEVELOPMENT (LIFE SCIENCE DIV)
1	DEPUTY CHIEF OF STAFF FOR MILITARY OPERATIONS (DGM)
1	DEPUTY CHIEF OF STAFF FOR MILITARY OPERATIONS (CBR)
1	OFFICE OF ASSISTANT CHIEF OF STAFF, G-2
1	CHIEF OF ENGINEERS (ENGMC-DE)
1	CHIEF OF ENGINEERS (ENGCW)
1	CG ARMY MATERIEL COMMAND (AMCRD-DE-NE)
1	U S ARMY EDGEWOOD ARSENAL
1	CG, COMBAT DEVELOPMENT COMMAND CBR AGENCY
1	COMMANDANT, CHEMICAL CORPS SCHOOLS (LIBRARY)
1	CO, CHEMICAL RESEARCH AND DEVELOPMENT LABORATORIES
1	COMMANDER, NUCLEAR DEFENSE LABORATORY
1	HQ, ARMY ENVIRONMENTAL HYGIENE AGENCY
1	CG, ABERDEEN PROVING GROUND
1	DIRECTOR, WALTER REED ARMY MEDICAL CENTER
1	CG, COMBAT DEVELOPMENTS COMMAND (CDCMR-V)
1	CG, QUARTERMASTER RES AND ENG COMMAND
1	HQ, DUGWAY PROVING GROUND
3	THE SURGEON GENERAL (MEDNE)
1	CO, ARMY ELECTRONIC RES AND DEV AGENCY
1	CG, ARMY ELECTRONIC PROVING GROUND
1	CO, ENGINEER RES AND DEV LABORATORY
1	DIRECTOR, USACDS NUCLEAR GROUP
1	CG, MOBILITY COMMAND
1	CG, MUNITIONS COMMAND
1	CG, FRANKFORD ARSENAL
1	CG, ARMY MISSILE COMMAND

AIR FORCE

1	ASSISTANT CHIEF OF STAFF(INTELLIGENCE AFCIN-3B)
6	CG, AERONAUTICAL SYSTEMS DIVISION (ASAPRD-NS)
1	DIRECTOR, USAF PROJECT RAND
1	COMMANDANT, SCHOOL OF AEROSPACE MEDICINE, BROOKS AFB
1	OFFICE OF THE SURGEON (SUP3.1), STRATEGIC AIR COMMAND
1	OFFICE OF THE SURGEON GENERAL
1	CG, SPECIAL WEAPONS CENTER (SWRB)
1	DIRECTOR, AIR UNIVERSITY LIBRARY, MAXWELL AFB
2	COMMANDER, TECHNICAL TRAINING WING, 3415TH TTG
1	HQ, SECOND AIRFORCE, BARKSDALE AFB
1	COMMANDER, ELECTRONIC SYSTEMS DIVISION (CRZT)

OTHER DOD ACTIVITIES

3	CHIEF, DEFENSE ATOMIC SUPPORT AGENCY (LIBRARY)
1	COMMANDER,FC/DASA, SANDIA BASE (FCDV)
1	COMMANDER, FC/DASA, SANDIA BASE (FCTG5, LIBRARY)
1	COMMANDER, FC/DASA, SANDIA BASE (FCWT)
2	OFFICE OF CIVIL DEFENSE, WASHINGTON
2	CIVIL DEFENSE UNIT, ARMY LIBRARY
20	DEFENSE DOCUMENTATION CENTER
1	DIRECTOR, ARMED FORCES RADIOBIOLOGY RESEARCH INSTITUTE

AEC ACTIVITIES AND OTHERS

1	AEC, DIVISION OF MILITARY APPLICATION
1	AEC SCIENTIFIC REPRESENTATIVE, FRANCE
1	AEROJET GENERAL, AZUSA
1	AEROJET GENERAL, SAN RAMON
1	ALLIS-CHALMERS MANUFACTURING CO, MILWAUKEE
1	ALLIS-CHALMERS MANUFACTURING CO, WASHINGTON
1	ALLISON DIVISION - GMC
2	ARGONNE CANCER RESEARCH HOSPITAL
10	ARGONNE NATIONAL LABORATORY
1	ATOMIC BOMB CASUALTY COMMISSION
3	ATOMIC ENERGY COMMISSION, WASHINGTON
4	ATOMIC ENERGY OF CANADA, LIMITED
4	ATOMICS INTERNATIONAL
1	BABCOCK AND WILCOX COMPANY
2	BATTELLE MEMORIAL INSTITUTE
2	BEERS, ROLAND F, INC
1	BERYLLIUM CORPORATION
4	BROOKHAVEN NATIONAL LABORATORY
1	BUREAU OF MINES, SALT LAKE CITY
1	BUREAU OF MINE, ALBANY
1	CARNEGIE INSTITUTE OF TECHNOLOGY
1	CHICAGO PATENT GROUP
1	COLUMBIA UNIVERSITY (HAVENS)
1	COLUMBIA UNIVERSITY (ROSSI)
1	COMBUSTION ENGINEERING, INC
1	COMBUSTION ENGINEERING, INC (NRD)
1	COMMITTEE ON THE EFFECTS OF ATOMIC RADIATION
5	DEFENCE RESEARCH MEMBER
1	DENVER RESEARCH INSTITUTE
1	DOW CHEMICAL COMPANY, ROCKY FLATS
4	DU PONT COMPANY, AIKEN

1	DU PONT COMPANY WILMINGTON
1	EDGERTON, GERMESHAUSEN AND GRIER, INC, GOLETA
1	EDGERTON, GERMESHAUSEN AND GRIER, INC, LAS VEGAS
1	FRANKLIN INSTITUE OF PENNSYLVANIA
1	FUNDAMENTAL METHODS ASSOCIATION
1	GENERAL ATOMIC DIVISION
1	GENERAL DYNAMICS-ASTRONAUTICS (NASA)
2	GENERAL DYNAMICS, FORT WORTH
2	GENERAL ELECTRIC COMPANY, CINCINNATI
4	GENERAL ELECTRIC COMPANY, RICHLAND
1	GENERAL ELECTRIC COMPANY, SAN JOSE
1	GENERAL ELECTRIC COMPANY, ST PETERSBURGH
1	GENERAL NUCLEAR ENGINEERING COPRORATION
1	GENERAL SCIENTIFIC CORPORATION
1	GIBBS AND COX, INC
1	GOODYEAR ATOMIC CORPORATION
1	HUGHES AIRCRAFT COMPANY, CULVER CITY
1	IOWA STATE UNIVERSITY
1	JET PROPULSION LABORATORY
2	KNOLLS ATOMIC POWER LABORATORY
1	LOCKHEED-GEORGIA COMPANY
1	LOCKHEED MISSILES AND SPACE COMPANY (NASA)
2	LOS ALAMOS SCIENTIFIC LABORATORY (LIBRARY)
1	MASSACHUSETTS INSTITUTE OF TECHNOLOGY (LINCOLN LAB)
1	LOS ALAMOS SCIENTIFIC LABORATORY (LIBRARY)
1	LOVELACE FOUNDATION
1	MARITIME ADMINISTRATION
1	MARTIN-MARIETTA CORPORATION
2	MIDWESTERN UNIVERSITIES RESEARCH ASSOCIATION
1	MOUND LABORATORY
1	NASA, LEWIS RESEARCH CENTER
2	NASA, SCIENTIFIC AND TECHNICAL INFORMATION FACILITY
1	NATIONAL BUREAU OF STANDARDS (LIBRARY)
1	NATIONAL BUREAU OF STANDARDS (TAYLOR)
1	NATIONAL LEAD COMPANY OF OHIO
2	NEVADA OPERATIONS OFFICE
1	NEW BRUNSWICK AREA OFFICE
1	NEW YORK OPERATIONS OFFICE
1	NUCLEAR MATERIALS AND EQUIPMENT CORPORATION
1	NUCLEAR METALS, INC
1	OFFICE OF ASSISTANT GENERAL GENERAL COUNSIL FOR PATENTS
4	PHILLIPS PETROLEUM COMPANY
1	POWER REACTOR DEVELOPMENT COMPANY
2	PRATT AND WHITNEY AIRCRAFT DIVISION
1	PRINCETON UNIVERSITY (WHITE)
1	PUBLIC HEALTH SERVICE, LAS VEGAS
1	PUBLIC HEALTH SERVICE, MONTGOMERY
2	PUBLIC HEALTH SERVICE, WASHINGTON
1	RESEARCH ANALYSIS CORPORATION
1	RENSSELAER POLYTECHNIC INSTITUTE
1	REYNOLDS ELECTRICAL AND ENGINEERING COMPANY, INC
1	SANDIA CORPORATION, ALBUQUERQUE
1	SANDIA CORPORATION (DOCUMENT ROOM)
1	SANDIA CORPORATION, LIVERMORE
1	SPACE TECHNOLOGY LABORATORIES, INC (NASA)
1	STANFORD UNIVERSITY (SLAC)
1	STATES MARINE LINES, INC
1	SYLVANIA ELECTRIC PRODUCTS, INC
1	TENNESSEE VALLEY AUTHORITY
2	UNION CARBIDE NUCLEAR COMPANY (ORGDP)
6	UNION CARBIDE NUCLEAR COMPANY (ORNL)
1	UNION CARBIDE NUCLEAR COMPANY (PADUCAH PLANT)
1	UNITED NUCLEAR CORPORATION (NDA)

1	UNIVERSITY OF CALIFORNIA, SAN FRANCISCO
1	UNIVERSITY OF CALIFORNIA, LOS ANGELES
2	U. OF CALIFORNIA LAWRENCE RADIATION LAB, BERKELEY
2	U. OF CALIFORNIA LAWRENCE RADIATION LAB, LIVERMORE
1	UNIVERSITY OF CHICAGO RADIATION LABORATORY
1	UNIVERSITY OF HAWAII
1	UNIVERSITY OF PUERTO RICO
1	UNIVERSITY OF ROCHESTER (ATOMIC ENERGY PROJECT)
1	UNIVERSITY OF ROCHESTER (MARSHAK)
1	UNIVERSITY OF UTAH
1	UNIVERSITY OF WASHINGTON (GEBALLE)
1	UNIVERSITY OF WASHINGTON (ROHDE)
1	US GEOLOGICAL SURVEY, DENVER
1	US GEOLOGICAL SURVEY, MENLO PARK
1	US GEOLOGICAL SURVEY, WASHINGTON
1	WESTERN RESERVE UNIVERSITY (FRIEDELL)
1	WESTERN RESERVE UNIVERSITY (MAJOR)
4	WESTINGHOUSE BETTIS ATOMIC POWER LABORATORY
1	WESTINGHOUSE ELECTRIC CORPORATION (RAHILLY)
1	WESTINGHOUSE ELECTRIC CORPORATION (NASA)
1	YANKEE ATOMIC ELECTRIC COMPANY
25	TECHNICAL INFORMATION EXTENSION, OAK RIDGE
40	USNRDL Technical Information Division

DISTRIBUTION DATE: 12 August 1963

Naval Radiological Defense Laboratory
USNRDL-TR-654
SUPPLEMENTARY ESTIMATES OF RADIATION GEOMETRY AND ENERGY RESPONSE FOR USNRDL GAMMA-INTENSITY-TIME RECORDER (GITR) MODEL 103 by H. R. Rinnert 13 May 1963 41 p. tables illus. 7 refs. UNCLASSIFIED

Estimates of radiation response are presented for the Model 103 Gamma-Intensity-Time Recorder (GITR) as used at Operation Sunbeam. The GITR detector unit, consisting of two concentric ionization chambers, was mounted inside

(over)

1. Radiation measurement systems components.

I. Rinnert, H. R.
II. Title.
III. Title: Gamma-intensity-time recorder.

UNCLASSIFIED

the GITR recorder case and located 3 ft above ground level. GITR responses and their time-dependence were estimated for several idealized radiation source geometries and several calculated gamma energy spectra. Estimated response values are presented as fractions of the GITR's calibration-response to Cs^{137} radiation beamed at the top of the unmounted detector along its longitudinal axis.

The GITR responses to distributed sources with specified gamma energy spectra did not show a significant dependence upon the source geometries investigated. There is 95% confidence that 95% of the population of GITR responses will be within 12% of the overall average response of 1.16 for the high-range detector, and within 14% of the overall average response of 0.99 for the low-range detector, during the first 110 hours after fission.

UNCLASSIFIED

Naval Radiological Defense Laboratory
USNRDL-TR-654
SUPPLEMENTARY ESTIMATES OF RADIATION GEOMETRY AND ENERGY RESPONSE FOR USNRDL GAMMA-INTENSITY-TIME RECORDER (GITR) MODEL 103 by H. R. Rinnert 13 May 1963 41 p. tables illus. 7 refs. UNCLASSIFIED

Estimates of radiation response are presented for the Model 103 Gamma-Intensity-Time Recorder (GITR) as used at Operation Sunbeam. The GITR detector unit, consisting of two concentric ionization chambers, was mounted inside

(over)

1. Radiation measurement systems components.

I. Rinnert, H. R.
II. Title.
III. Title: Gamma-intensity-time recorder.

UNCLASSIFIED

the GITR recorder case and located 3 ft above ground level. GITR responses and their time-dependence were estimated for several idealized radiation source geometries and several calculated gamma energy spectra. Estimated response values are presented as fractions of the GITR's calibration-response to Cs^{137} radiation beamed at the top of the unmounted detector along its longitudinal axis.

The GITR responses to distributed sources with specified gamma energy spectra did not show a significant dependence upon the source geometries investigated. There is 95% confidence that 95% of the population of GITR responses will be within 12% of the overall average response of 1.16 for the high-range detector, and within 14% of the overall average response of 0.99 for the low-range detector, during the first 110 hours after fission.

UNCLASSIFIED

Naval Radiological Defense Laboratory
USNRDL-TR-654
SUPPLEMENTARY ESTIMATES OF RADIATION GEOMETRY AND ENERGY RESPONSE FOR USNRDL GAMMA-INTENSITY-TIME RECORDER (GITR) MODEL 103 by H. R. Rinnert 13 May 1963 41 p. tables illus. 7 refs. UNCLASSIFIED

Estimates of radiation response are presented for the Model 103 Gamma-Intensity-Time Recorder (GITR) as used at Operation Sunbeam. The GITR detector unit, consisting of two concentric ionization chambers, was mounted inside
(over)

1. Radiation measurement systems components.

I. Rinnert, H. R.
II. Title.
III. Title: Gamma-intensity-time recorder.

UNCLASSIFIED

Naval Radiological Defense Laboratory
USNRDL-TR-654
SUPPLEMENTARY ESTIMATES OF RADIATION GEOMETRY AND ENERGY RESPONSE FOR USNRDL GAMMA-INTENSITY-TIME RECORDER (GITR) MODEL 103 by H. R. Rinnert 13 May 1963 41 p. tables illus. 7 refs. UNCLASSIFIED

Estimates of radiation response are presented for the Model 103 Gamma-Intensity-Time Recorder (GITR) as used at Operation Sunbeam. The GITR detector unit, consisting of two concentric ionization chambers, was mounted inside
(over)

1. Radiation measurement systems components.

I. Rinnert, H. R.
II. Title.
III. Title: Gamma-intensity-time recorder.

UNCLASSIFIED

the GITR recorder case and located 3 ft above ground level. GITR responses and their time-dependence were estimated for several idealized radiation source geometries and several calculated gamma energy spectra. Estimated response values are presented as fractions of the GITR's calibration-response to Cs^{137} radiation beamed at the top of the unmounted detector along its longitudinal axis.

The GITR responses to distributed sources with specified gamma energy spectra did not show a significant dependence upon the source geometries investigated. There is 95% confidence that 95% of the population of GITR responses will be within 12% of the overall average response of 1.16 for the high-range detector, and within 14% of the overall average response of 0.99 for the low-range detector, during the first 110 hours after fission.

UNCLASSIFIED

the GITR recorder case and located 3 ft above ground level. GITR responses and their time-dependence were estimated for several idealized radiation source geometries and several calculated gamma energy spectra. Estimated response values are presented as fractions of the GITR's calibration-response to Cs^{137} radiation beamed at the top of the unmounted detector along its longitudinal axis.

The GITR responses to distributed sources with specified gamma energy spectra did not show a significant dependence upon the source geometries investigated. There is 95% confidence that 95% of the population of GITR responses will be within 12% of the overall average response of 1.16 for the high-range detector, and within 14% of the overall average response of 0.99 for the low-range detector, during the first 110 hours after fission.

UNCLASSIFIED

Naval Radiological Defense Laboratory
USNRDL-TR-654
SUPPLEMENTARY FSTIMATES OF RADIATION GEOMETRY AND ENERGY RESPONSE FOR USNRDL GAMMA-INTENSITY-TIME RECORDER (GITR) MODEL 103 by H. R. Rinnert 13 May 1963 41 p. tables illus. 7 refs. UNCLASSIFIED

Estimates of radiation response are presented for the Model 103 Gamma-Intensity-Time Recorder (GITR) as used at Operation Sunbeam. The GITR detector unit, consisting of two concentric ionization chambers, was mounted inside

(over)

1. Radiation measurement systems components.

I. Rinnert, H. R.
II. Title.
. Title: Gamma-intensity-time recorder.

UNCLASSIFIED

Naval Radiological Defense Laboratory
USNRDL-TR-654
SUPPLEMENTARY ESTIMATES OF RADIATION GEOMETRY AND ENERGY RESPONSE FOR USNRDL GAMMA-INTENSITY-TIME RECORDER (GITR) MODEL 103 by H. R. Rinnert 13 May 1963 41 p. tables illus. 7 refs. UNCLASSIFIED

Estimates of radiation response are presented for the Model 103 Gamma-Intensity-Time Recorder (GITR) as used at Operation Sunbeam. The GITR detector unit, consisting of two concentric ionization chambers, was mounted inside

(over)

1. Radiation measurement systems components.

I. Rinnert, H. R.
II. Title.
III. Title: Gamma-intensity-time recorder.

UNCLASSIFIED

the GITR recorder case and located 3 ft above ground level. GITR responses and their time-dependence were estimated for several idealized radiation source geometries and several calculated gamma energy spectra. Estimated response values are presented as fractions of the GITR's calibration-response to Cs^{137} radiation beamed at the top of the unmounted detector along its longitudinal axis.

The GITR responses to distributed sources with specified gamma energy spectra did not show a significant dependence upon the source geometries investigated. There is 95% confidence that 95% of the population of GITR responses will be within 12% of the overall average response of 1.16 for the high-range detector, and within 14% of the overall average response of 0.99 for the low-range detector, during the first 110 hours after fission.

UNCLASSIFIED

the GITR recorder case and located 3 ft above ground level. GITR responses and their time-dependence were estimated for several idealized radiation source geometries and several calculated gamma energy spectra. Estimated response values are presented as fractions of the GITR's calibration-response to Cs^{137} radiation beamed at the top of the unmounted detector along its longitudinal axis.

The GITR responses to distributed sources with specified gamma energy spectra did not show a significant dependence upon the source geometries investigated. There is 95% confidence that 95% of the population of GITR responses will be within 12% of the overall average response of 1.16 for the high-range detector, and within 14% of the overall average response of 0.99 for the low-range detector, during the first 110 hours after fission.

UNCLASSIFIED

Naval Radiological Defense Laboratory
USNRDL-TR-654
SUPPLEMENTARY ESTIMATES OF RADIATION GEOMETRY AND ENERGY RESPONSE FOR USNRDL GAMMA-INTENSITY-TIME RECORDER (GITR) MODEL 103 by H. R. Rinnert 13 May 1963 41 p. tables illus. 7 refs. UNCLASSIFIED

Estimates of radiation response are presented for the Model 103 Gamma-Intensity-Time Recorder (GITR) as used at Operation Sunbeam. The GITR detector unit, consisting of two concentric ionization chambers, was mounted inside
(over)

1. Radiation measurement systems components.

I. Rinnert, H. R.
II. Title.
III. Title: Gamma-intensity-time recorder.

UNCLASSIFIED

Naval Radiological Defense Laboratory
USNRDL-TR-654
SUPPLEMENTARY ESTIMATES OF RADIATION GEOMETRY AND ENERGY RESPONSE FOR USNRDL GAMMA-INTENSITY-TIME RECORDER (GITR) MODEL 103 by H. R. Rinnert 13 May 1963 41 p. tables illus. 7 refs. UNCLASSIFIED

Estimates of radiation response are presented for the Model 103 Gamma-Intensity-Time Recorder (GITR) as used at Operation Sunbeam. The GITR detector unit, consisting of two concentric ionization chambers, was mounted inside
(over)

1. Radiation measurement systems components.

I. Rinnert, H. R.
II. Title.
III. Title: Gamma-intensity-time recorder.

UNCLASSIFIED

the GITR recorder case and located 3 ft above ground level. GITR responses and their time-dependence were estimated for several idealized radiation source geometries and several calculated gamma energy spectra. Estimated response values are presented as fractions of the GITR's calibration-response to Cs^{137} radiation beamed at the top of the unmounted detector along its longitudinal axis.

The GITR responses to distributed sources with specified gamma energy spectra did not show a significant dependence upon the source geometries investigated. There is 95% confidence that 95% of the population of GITR responses will be within 12% of the overall average response of 1.16 for the high-range detector, and within 14% of the overall average response of 0.99 for the low-range detector, during the first 110 hours after fission.

UNCLASSIFIED

the GITR recorder case and located 3 ft above ground level. GITR responses and their time-dependence were estimated for several idealized radiation source geometries and several calculated gamma energy spectra. Estimated response values are presented as fractions of the GITR's calibration-response to Cs^{137} radiation beamed at the top of the unmounted detector along its longitudinal axis.

The GITR responses to distributed sources with specified gamma energy spectra did not show a significant dependence upon the source geometries investigated. There is 95% confidence that 95% of the population of GITR responses will be within 12% of the overall average response of 1.16 for the high-range detector, and within 14% of the overall average response of 0.99 for the low-range detector, during the first 110 hours after fission.

UNCLASSIFIED